Adaptive Communications and Signal Processing laboratory

Cornell University, Ithaca, NY 14853

Tracking of Fast-Fading Channels in Long Code WCDMA

Y. Sung and L. Tong

Technical Report No. ACSP-TR-11-02-03

November 2002

Abstract

A new technique for blind tracking of fast fading channels in long code CDMA is proposed by exploiting multipath diversity. Based on a linear interpolation channel model, the proposed method blindly identifies a time-varying channel at arbitrary estimating points within a block up to a scale factor and increases bandwidth efficiency allowing only one pilot symbol within a block which is much larger than channel coherence time. The proposed method can be implemented using an efficient state-space inversion technique for multiuser cases. The mean square error performance of the proposed estimator is compared with Cramér-Rao bound for interpolated channel. Modeling error and bit error rate are also evaluated using Monte-Carlo simulations, and compared with the block fading model and a decision-directed tracking technique.

Index Terms— Fast fading, Long code CDMA, Pilot symbols, Channel estimation and tracking, Interpolation.

EDICS: 3-CEQU (Channel modeling, estimation, and equalization).

I. Introduction

Recent code division multiple access (CDMA) systems adopt coherent detection schemes in forward and reverse links. The coherent demodulation is shown to provide better system performance than the noncoherent detection using orthogonal signaling or differential decoding in CDMA systems [1] and in narrowband systems [2] [3]. Channel estimation plays a crucial role in coherent detection. To estimate the channel variation in a fading environment, usually pilot symbols are periodically inserted in time-division multiplexing (TDM) or the reference code channel is superimposed on data channel by code-division multiplexing (CDM). Although the continuous code-division multiplexed reference channel is more attractive for channel tracking, it increases the peak-to-average power ratio of the transmitter, which reduces the energy efficiency. The insertion of pilot symbols in a time-division manner mitigates the peak-to-average power ratio increase.

Several channel tracking methods have been proposed based on time multiplexed pilot symbols and interpolation techniques for CDMA systems, e.g. [4] [5]. These methods estimate the channel with low implementation complexity. However, the pure training-based schemes require frequently inserted pilot symbols with high SNR since they utilize only pilot symbols. Usually, pilot clusters are placed so that the pilot repetition period is smaller than the channel coherence time. The frequent pilot symbols reduce the bandwidth efficiency of transmission.

To handle this problem, many authors have proposed blind or semi-blind estimation methods based on various techniques such as direct inversion, subspace, and second-order moment method [10] [11] [12] [13]. These methods utilize not only the pilot but the structure of the unknown data symbols to eliminate the necessity of a large amount of pilot symbols. However, they are based on the block fading assumption that is not valid for fast fading channels where channel changes rapidly within a block, which requires the division of a block into smaller ones and additional pilot insertion in the subblock to resolve the inherent scalar ambiguity of blind methods.

Iterative methods based on maximum likelihood (ML) principle have also proposed. Several authors proposed methods based on expectation-maximization (EM) technique [6] [7], or semi-blind ML approach [8]. These iterative methods are based on the slow fading assumption and often suffer from well-known problems such as local convergence and high complexity. In [9], the authors proposed an efficient channel estimation method based on LMS-like iteration for an approximate ML solution with training sequence. Though the proposed method tracks a slowly time-varying channel utilizing previously detected symbols, its performance depends on the size of the training preamble and the repetition of training clusters which usually reduces the bandwidth efficiency.

In this paper, we propose a new blind tracking technique for fast-fading long code CDMA systems with slotted transmissions where the slot size is larger than the channel coherence time. Based on a linear interpolation model, the proposed method exploits the multi-path diversity of mobile channels and estimates the channel coefficients at the selected estimating points which are located arbitrarily within a block. The use of interpolation model converts the time-varying channel parameters to fixed parameters associated with the block and often makes blind estimation approaches tractable in time-varying channels [16]. The proposed scheme consists of front end processing and blind identification of a parameter matrix which is associated with the estimating points. The elimination of unknown symbols is based on the cross referencing [17]. A new identifiability is established for noiseless case and new detection schemes are proposed based on the estimated parameter matrix. For multiuser scenario, decorrelating or regularized decorrelating front end can be used. The fast inversion of code matrix can be implemented with a state-space

technique with a comparable amount of complexity with short code CDMA cases [13].

The data model of a CDMA system is described and linear interpolation model is introduced in Section II. Section III presents a blind channel tracking method and detection schemes based on the proposed estimation. The bit error rate of the proposed algorithm is analyzed in Section IV. In Section V, the performance of the proposed method is evaluated through Cramér-Rao bound and Monte Carlo simulations and compared with the block fading model and a decision-directed tracking scheme. Lastly, we briefly discuss several issues related to the proposed algorithm.

A. Notation

The notations are standard. Vectors and matrices are written in boldface with matrices in capitals. We reserve $\mathbf{I}_m$ for the identity matrix of size m (the subscript is included only when necessary). For a random vector $\mathbf{x}$, $\mathbb{E}(\mathbf{x})$ is the statistical expectation of $\mathbf{x}$. The notation $\mathbf{x} \sim \mathcal{N}(\boldsymbol{\mu}, \boldsymbol{\Sigma})$ means that $\mathbf{x}$ is (complex) Gaussian with mean $\boldsymbol{\mu}$ and covariance $\boldsymbol{\Sigma}$. For a scalar α, α^* denotes the complex conjugate of α. Operations $(\cdot)^T$ and $(\cdot)^H$ indicate transpose and Hermitian transpose, respectively. $\mathrm{diag}(\mathbf{X}_1, \ldots, \mathbf{X}_N)$ is a block diagonal matrix with $\mathbf{X}_1, \ \ldots, \ \mathbf{X}_N$ as its diagonal blocks. Given a matrix $\mathbf{X}$, $\mathbf{X}^\dagger$ is the Moore-Penrose pseudo inverse. For a matrix (vector) $\mathbf{X}$, we use $\|\mathbf{X}\|$ for the 2-norm.

II. Data Model

A. System Model

We consider a long code CDMA system with K asynchronous users. At the transmitter, a particular user i transmits M_i symbols $\{s_{im}, m = 1, \ldots, M_i\}$ in each slot and each symbol s_{im} is spread by an aperiodic code vector $\mathbf{c}_{im}$ with spreading gain G_i, followed by a chip pulse-shaping filter. We assume that the spreading codes are deterministic and known to the receiver and also regard the data symbol $\{s_{im}\}$ as deterministic parameter.

We assume that the propagation channel of user i consists of L_i independent multipaths and each is a bandlimited waveform with bandwidth f_D [22] . We let the multipath coefficients vary from symbol to symbol while remaining constant over one symbol period T_s. We assume that the rough timing of multipath cluster is known and all users are

chiprate synchronized[1], that is, the delays between paths are multiples of chip interval T_c. Specifically, the continuous time-varying channel impulse response of user i is given by

$$h_i(t,\tau) = \sum_{l=1}^{L_i} h_i^{(l)}(t)\delta(\tau - D_i^{(l)}T_c), \tag{1}$$

where $h_i^{(l)}(t)$ is the complex coefficient waveform for the lth path and $D_i^{(l)}$ the delay of the lth path of user i relative to the slot reference at the receiver. The propagation channel at the mth symbol duration of user i can be modeled by a finite impulse response as

$$\mathbf{h}_{im} \triangleq \left[h_{im}^{(1)}, \cdots, h_{im}^{(L_i)}\right]^T, \tag{2}$$

where $h_{im}^{(l)} \triangleq h_i(mT_s, D_i^{(l)}T_c),\ l = 1, \ldots, L_i$.

Let the received signal corresponding to symbol s_{im} be passed through a chip-matched filter and sampled synchronously at the chip rate. Let $\mathbf{y}_{im}$ be the vector of the chiprate received samples, and $\mathbf{y}_{im}$ is a linear combination of shifted (delayed) code vectors $\mathbf{c}_{im}$. Here $\mathbf{c}_{im}$ is the segment of G_i chips of user i's spreading code corresponding to the mth symbol. Each shifted code vector is multiplied by the lth fading coefficient $h_{im}^{(l)}$, and the channel response $\mathbf{y}_{im}$ to s_{im} is given by

$$\mathbf{y}_{im} = \mathbf{T}_{im}\mathbf{h}_{im}s_{im}. \tag{3}$$

Here, $\mathbf{T}_{im}$ is the code matrix of user i and symbol m (see Fig. 1), and $\mathbf{h}_{im}$ is the multipath channel vector for user i at time mT_s.

Since the channel is linear, the total received noiseless signal for user i is given by

$$\begin{aligned} \mathbf{y}_i &= \sum_{m=1}^{M_i} \mathbf{T}_{im}\mathbf{h}_{im}s_{im}, &(4)\\ &= \mathbf{T}_i \mathrm{diag}(\mathbf{h}_{i1}, \cdots, \mathbf{h}_{iM_i})\mathbf{s}_i, \\ \mathbf{T}_i &\triangleq [\mathbf{T}_{i1}, \cdots, \mathbf{T}_{iM_i}], &(5) \end{aligned}$$

where $\mathbf{T}_i$ is the code matrix of user i and it does not depend on the gains and phases of the multipath channel. Now including K' ($\leq K$) users of interest and the noise, we have

$$\mathbf{y} = \mathbf{THs} + \mathbf{w}, \tag{6}$$

[1]With Nyquist sampling the exact chiprate sampling is not required. The derivation here will correspond to the even (or odd) subsequence of a $T_c/2$ sampled observation.

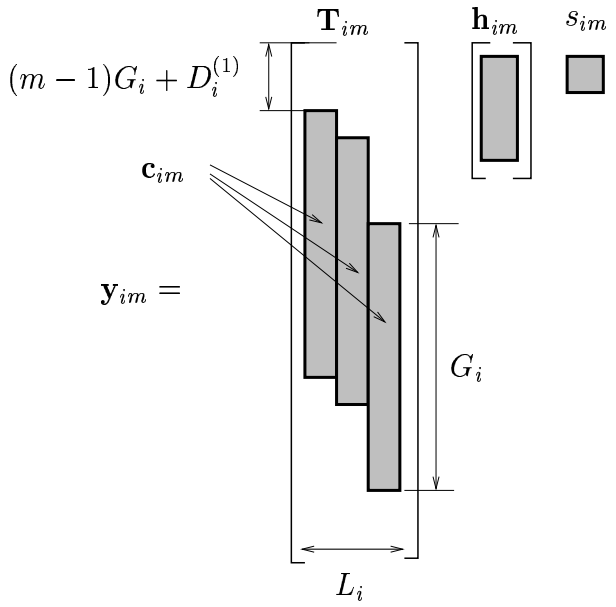

Fig. 1. Code matrix for one symbol

$$\begin{aligned} \mathbf{T} &\triangleq [\mathbf{T}_1, \cdots, \mathbf{T}_{K'}], \\ \mathbf{H} &\triangleq \mathrm{diag}(\mathbf{h}_{11}, \cdots, \mathbf{h}_{1M_1}, \mathbf{h}_{21}, \cdots, \mathbf{h}_{2M_2}, \mathbf{h}_{31}, \cdots, \mathbf{h}_{K'M_{K'}}), \end{aligned} \tag{7}$$

where $\mathbf{H}$ is a block diagonal matrix with $\mathbf{h}_{im}$ as its diagonal blocks, $\mathbf{s}$ a vector stacking all users' symbol vectors, and $\mathbf{w}$ a vector representing the additive Gaussian noise.

We assume the following

(A1): The code matrix $\mathbf{T}$ is known and has full column rank.

(A2): The noise vector is circularly symmetric complex Gaussian $\mathbf{w} \sim \mathcal{N}(\mathbf{0}, \sigma^2\mathbf{I})$ with possibly unknown σ^2.

Assumption (A1) implies that the receiver knows the codes, delay offset $D_i^{(l)}$, and the number of fingers L_i of all users in the signal part of (6). This assumption is usually valid for the uplink. The full column assumption is easily satisfied with reasonably high spreading gains or properly chosen K'. For an example of equal spreading gains and equal channel lengths, K' is determined to satisfy $LK' \leq G$. One way of choosing K' users is to include the desired user and several others with the largest interference power and all the rest user signals are assumed to be Gaussian and put in noise vector $\mathbf{w}$. This is possible since the signal-to-noise ratio for each user is available in the uplink. In the case of $K' < K$, several parallel receivers with different set of users can be used to demodulate

all users. L_i is a model parameter which is often left to system designers.

B. Linear Interpolation Channel Model

We consider a linear interpolation channel model under the deterministic parameter assumption. Linear interpolation is used for the problem of signal reconstruction using an infinite or finite number of samples by many authors [19] [20]. The interpolation model reduces the number of parameters of a time-varying channel using a set of interpolation coefficients. For the case of batch operation, the interpolation model converts the time-varying channel parameters within a block to time-invariant parameters such as parameters associated with selected estimating points or basis, which often makes blind estimation approaches tractable, e.g., [16]. For the frequency-domain approach, each path of a channel can be represented as a weighted sum of complex exponentials. Due to the bandwidth expansion by slot truncation, the frequency-domain approach requires a much larger number of parameters than the time-domain case to obtain a comparable performance. We focus on the time-domain approach.

B.1 Time-domain Approach

We consider a N sample time-domain approach which includes a broad range of interpolation techniques such as piecewise linear, polynomial, ideal lowpass, optimal time-invariant and time-varying least squares interpolations.

We assume that the channel at a specific time within a slot is a linear combination of channel coefficients at N estimating points. Consider the channel of user i. Let $g_{in}^{(l)}, n = 1, 2, \ldots, N$, denote the channel coefficient at the nth estimating point for the lth path of user i. The channel $h_{im}^{(l)}$ at the mth symbol interval is given by

$$h_{im}^{(l)} = \alpha_{m1} g_{i1}^{(l)} + \alpha_{m2} g_{i2}^{(l)} \cdots + \alpha_{mN} g_{iN}^{(l)}, \quad m = 1, \cdots, M_i, \tag{8}$$

where α_{mn} is the interpolation coefficient for symbol m and sample n. Stacking all the multipaths corresponding to the same symbol interval for the same user gives

$$\mathbf{h}_{im} \triangleq \begin{bmatrix} h_{im}^{(1)} \\ \vdots \\ h_{im}^{(L_i)} \end{bmatrix} = \mathbf{G}_i \mathbf{a}_m, \tag{9}$$

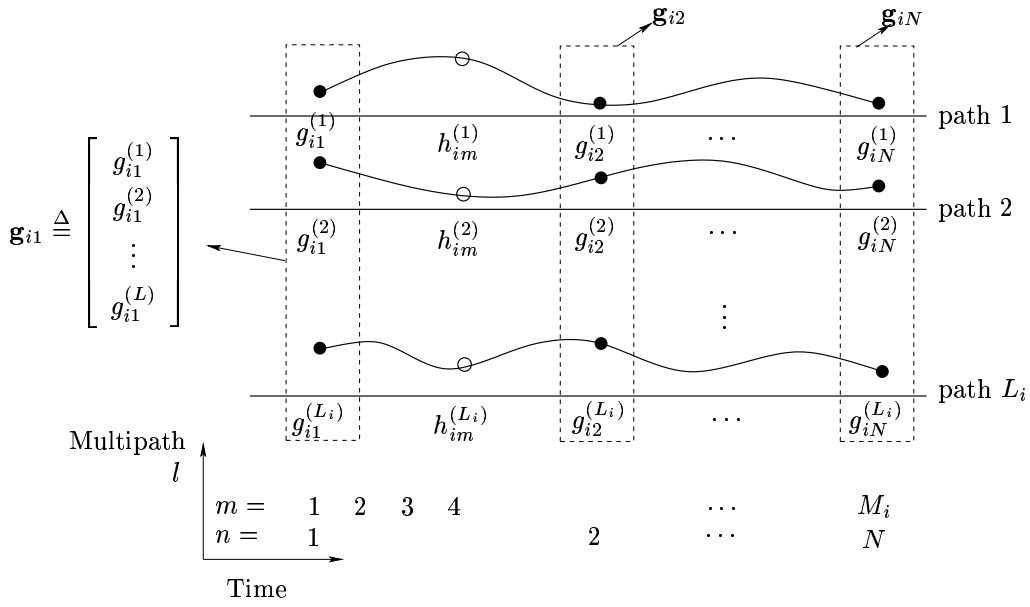

Fig. 2. Linear interpolation multipath channel model

where $\mathbf{a}_m \triangleq [\alpha_{m1}, \alpha_{m2}, \cdots, \alpha_{mN}]^T$ and

$$\begin{aligned} \mathbf{G}_i &\triangleq \begin{bmatrix} g_{i1}^{(1)} & g_{i2}^{(1)} & \cdots & g_{iN}^{(1)} \\ g_{i1}^{(2)} & g_{i2}^{(2)} & \cdots & g_{iN}^{(2)} \\ \vdots & & & \vdots \\ g_{i1}^{(L_i)} & g_{i2}^{(L_i)} & \cdots & g_{iN}^{(L_i)} \end{bmatrix}, \qquad (10) \\ &= [\mathbf{g}_{i1}, \mathbf{g}_{i2}, \cdots, \mathbf{g}_{iN}], \\ \mathbf{g}_{in} &\triangleq [g_{in}^{(1)}, g_{in}^{(2)}, \cdots, g_{in}^{(L_i)}]^T \qquad (11) \end{aligned}$$

for $n = 1, 2, \cdots, N$. The interpolation coefficient vector $\mathbf{a}_m$ is determined by the interpolation function and the matrix $\mathbf{G}_i$ contains the unknown channel parameters at the selected estimating points.

We further assume the following

(A3): The matrix $\mathbf{G}_i$ has full column rank.

Assumption (A3) implies that the number of multipaths is larger than or equal to that of the estimating points. Due to the abundance of the multipaths in wireless channels, this assumption can be easily satisfied with the proper selection of the the number of estimating points N. The number of estimating points N is a design parameter which is selected,

possibly in an adaptive way, considering the fading rate so that the channel vectors at different estimating points are linearly independent almost surely.[2] If we select two end points of slot as the estimating points with pilot symbol placement at each end, the model can be considered as the common interpolation based on the pilot symbols. When N is one, the interpolation model reduces to the general block fading model. One way to guarantee that we place several estimating points within a slot is to use multiple receive antennas at the base station which is common in actual uplink designs. The multiple receive antennas provide multipath diversity to exploit. In this case, the proposed method can be used to jointly estimate the time-varying channel of each antenna.

C. Optimal Least-Square Interpolation

Sampling theorem ensures the exact reconstruction for a bandlimited signal with an infinite number of samples. Even though the channel for a particular path is bandlimited by the Doppler frequency f_D, truncation of channel for slot interval increases the bandwidth to infinity which requires an infinite number of samples within a slot. Due to the multipath structure of mobile transmissions, a finite number of samples are available for the proposed algorithm to reconstruct channel. The ideal lowpass interpolation is not optimal in this case and there exists an inherent approximation error[3] for interpolation with a finite number of samples which gives rise to the problem of optimal reconstruction from finite data samples.

The optimal design of the interpolation function requires some statistical knowledge of channel such as power spectral density which is be usually modeled as ideal lowpass or Jakes's spectrum with bandwidth f_D [22]. Suppose that the channel waveform $h(t)$-we abbreviate the indexes for user and multipath- is a realization of a wide-sense stationary random process with bandwidth f_D[4]. The optimal interpolation problem is stated as follows. For a given random waveform $h(t)$ and its samples $h(t_n)$ at time instant

[2]The overparameterization of N makes the parameter matrix $\mathbf{G}_i$ poorly conditioned which induces severe noise enhancement in step (28) for noisy cases.

[3]The perturbation to interpolation due to the noisy samples and truncation is well analyzed in [21].

[4]Though our channel assumption is a deterministic for a given slot, the channel waveform of each slot can be assumed to be a realization of random process with finite bandwidth. Since the interpolation coefficients are to be determined regardless of slot, the interpolation function is optimized with respect to all possible realizations of channel waveform.

$\{t_n\}_{n=1,2,...,N} \in [0,\ T_{slot}]$, the waveform $h(t)$ is approximated by a linear combination of interpolation functions $i_n(t)$ as

$$\hat{h}(t) = \sum_{n=1}^{N} h(t_n) i_n(t), \quad 0 \le t \le T_{slot} \tag{12}$$

such that it minimizes the mean square error ϵ defined as

$$\epsilon = \int_0^{T_{slot}} \mathbb{E}\ |h(t) - \hat{h}(t)|^2 dt \tag{13}$$

We consider the periodic sampling. The sampling instants are given as $t_n = (n-1)T,\ n = 1, \ldots, N$ for a period T. The optimal interpolation function $i_n(t)$ can be obtained using a variational technique and is given by the solution of the following linear equations [18] [19]

$$R_h(\tau - kT) = \sum_{n=0}^{N-1} R_h((k-n)\tau) i_{n+1}(\tau) \quad \text{for } k = 0, 1, \cdots, N-1$$

with $0 \le \tau \le (N-1)T$ where $R_h(\tau)$ is the autocorrelation function of $h(t)$.

The time-invariant case is optimized with an additional constraint on the interpolation function $i_n(t)$, that is,

$$i(t) = i_n(t) \quad \text{for all} \quad n = 1, \cdots, N. \tag{14}$$

A similar variational technique can be used for the optimization in the time-invariant case and the solution is determined by a set of linear equations [19] [20]. Since the time-invariant optimization is a subset of time-varying optimization, the optimal time-varying interpolation always shows a better mean square error performance over the time-invariant case.

C.1 Frequency-domain Approach

As in the time-domain case, we can model the channel as a linear combination of finite terms in the frequency-domain approach, where channel is represented as a weighted sum of complex exponentials. We assume that the channel waveform for each path is bandlimited with Doppler bandwidth f_D [22]. Due to the truncation for slot interval, the channel waveform is not strictly bandlimited. However, when the slot length is much larger than the channel coherence time, the channel can be still modeled as bandlimited. Specifically,

using DFT, the channel for one slot period of user i's path l can be modeled as

$$h_{im}^{(l)} = \sum_{k=0}^{M_i-1} H_{ik}^{(l)} \exp(j2\pi \frac{(m-1)k}{M_i}), \ m = 1, \ldots, M_i, \tag{15}$$

where $H_{ik}^{(l)}$ is DFT coefficient of $h_{im}^{(l)}$.

The frequency offset between DFT coefficients is given as

$$\Delta f = \frac{1}{M_i T_s}. \tag{16}$$

Since the channel is almost bandlimited, we can approximate the channel as a finite sum

$$\tilde{h}_{im}^{(l)} = \sum_{k \in \mathcal{K}} H_{ik}^{(l)} \exp(j2\pi \frac{(m-1)k}{M_i}), \tag{17}$$

where $\mathcal{K} \triangleq \{0, 1, \ldots, N/2, M_i - N/2, \ldots, M_i - 1\}$ and $N/2 = \lceil \frac{f_D}{\Delta f} \rceil$. $\mathbf{g}_i$ and α_{mn} are given as

$$g_{in(k)}^{(l)} = H_{ik}^{(l)}, \quad \alpha_{mn(k)} = \exp(j2\pi \frac{(m-1)k}{M_i}), \quad k \in \mathcal{K}. \tag{18}$$

where $n(k)$ is a one-to-one index function from $\mathcal{K}$ to $\{1, 2, \ldots, N\}$. For frequency-domain approach, a larger number of parameters are usually required to give a comparable modeling than the time-domain case.

III. Blind Channel Tracking Algorithm

In this section, we propose a blind estimator for an equalizer based on a linear interpolation model exploiting the multipath diversity of propagation channel. The proposed algorithm is based on the cross reference technique to eliminate the unknown data symbols [17].

A. Front-end processing

We consider the conventional matched filter, decorrelator, and regularized decorrelator as the front end. The regularized decorrelator can be used to mitigate the noise enhancement for an improved performance. When the spreading factor is large and the multiuser interference is not severe, the conventional matched filter (Hermitian of the code matrix) can be used without a significant performance loss. The complexity of these front ends is briefly discussed in Section III-D.

The output $\mathbf{z}$ of the decorrelating front end is given by

$$\mathbf{z} = \mathbf{T}^{\dagger}\mathbf{y}. \tag{19}$$

Here, $\mathbf{T}^H$ and $(\mathbf{T}^H\mathbf{T} + \sigma^2\mathbf{I})^{-1}\mathbf{T}^H$ can be used instead of the pseudo-inverse $\mathbf{T}^{\dagger}$ for the conventional matched filter and the regularized decorrelator, respectively. Let $\mathbf{z}_{im}$ denote the $L_i \times 1$ subvector of $\mathbf{z}$ corresponding to the mth symbol of user i. Due to the block diagonal structure of $\mathbf{H}$ in (6), the vector $\mathbf{z}_{im}$ is given by

$$\begin{aligned} \mathbf{z}_{im} &= \mathbf{h}_{im}s_{im} + \mathbf{n}_{im}, \\ &= \mathbf{G}_i\mathbf{a}_m s_{im} + \mathbf{n}_{im}, \quad m = 1, \ldots, M_i, \end{aligned} \tag{20}$$

where the vector $\mathbf{a}_m$ is known and determined by the selected interpolation method and $\mathbf{n}_{im}$ has distribution of $\mathcal{N}(\mathbf{0}, \sigma^2\mathbf{\Sigma}_{im})$. For the decorrelating front end, $\mathbf{n}_{im}$ is from the additive noise $\mathbf{w}$ in (6) and its covariance $\mathbf{\Sigma}_{im}$ is the $L_i \times L_i$ submatrix obtained from the $(i-1)M + m$th diagonal block of $\mathbf{T}^{\dagger}(\mathbf{T}^{\dagger})^H$ for the case of equal spreading gain and slot size among users. For the case of conventional matched filter, the noise contains both the additive noise and Gaussian modeled other user interference. Note that the output of the front end are multiple observations related to the same unknown parameter $\mathbf{G}_i$ due to the interpolation channel model.

B. Algorithm Construction

B.1 Noiseless case

Consider the noiseless case with the decorrelating front end where the observation vector is given by

$$\mathbf{z}_{im} = \mathbf{G}_i\mathbf{a}_m s_{im}, \quad m = 1, \ldots, M_i. \tag{21}$$

First, we obtain the column space of $\mathbf{G}_i$ by the following singular value decomposition

$$\mathbf{Z}_i = \mathbf{U}_i\mathbf{S}_i\mathbf{V}_i^H, \tag{22}$$

where $\mathbf{Z}_i$ is defined as

$$\mathbf{Z}_i \triangleq [\mathbf{z}_{i1}, \mathbf{z}_{i2}, \ldots, \mathbf{z}_{iM_i}], \tag{23}$$

$$= \mathbf{G}_i[\mathbf{a}_1 s_{i1}, \cdots, \mathbf{a}_{M_i} s_{iM_i}]. \tag{24}$$

Since $\mathbf{U}_i$ and $\mathbf{G}_i$ span the same subspace, we can factorize $\mathbf{G}_i$ as

$$\mathbf{G}_i = \mathbf{U}_i \Gamma_i, \tag{25}$$

where Γ_i is an unknown $N \times N$ square matrix. Projecting the vector $\mathbf{z}_{im}$ to the subspace $\mathbf{U}_i$ gives

$$\mathbf{x}_{im} \stackrel{\Delta}{=} \mathbf{U}_i^H \mathbf{z}_{im} = \Gamma_i \mathbf{a}_m s_{im}. \tag{26}$$

Now, we have a system of equations with square matrix Γ_i. Since $\mathbf{G}_i$ has full column rank by the assumption *(A3)*, Γ_i is invertible. Let $\mathbf{W}_i^H$ be the inverse of Γ_i and have a row partition as

$$\mathbf{W}_i^H = \begin{bmatrix} \mathbf{w}_{i1}^H \\ \mathbf{w}_{i2}^H \\ \vdots \\ \mathbf{w}_{iN}^H \end{bmatrix}. \tag{27}$$

Applying the inverse of Γ_i to $\mathbf{x}_{im}$ gives

$$\mathbf{W}_i^H \mathbf{x}_{im} = \begin{bmatrix} \mathbf{w}_{i1}^H \mathbf{x}_{im} \\ \mathbf{w}_{i2}^H \mathbf{x}_{im} \\ \vdots \\ \mathbf{w}_{iN}^H \mathbf{x}_{im} \end{bmatrix} = \begin{bmatrix} \alpha_{m1} s_{im} \\ \alpha_{m2} s_{im} \\ \vdots \\ \alpha_{mN} s_{im} \end{bmatrix}. \tag{28}$$

Notice that each row is a product of a known scalar α_{mn} and an unknown common data symbol s_{im}. Multiplying row j, k by α_{mk}, α_{mj} respectively gives the same value $\alpha_{mj}\alpha_{mk}s_{im}$. Taking difference between two rows related to mth symbol, we obtain a system of equations similarly as in [17].

$$\begin{aligned}
\mathbf{w}_{i1}^H \alpha_{m2} \mathbf{x}_{im} - \mathbf{w}_{i2}^H \alpha_{m1} \mathbf{x}_{im} &= 0 \\
\mathbf{w}_{i1}^H \alpha_{m3} \mathbf{x}_{im} - \mathbf{w}_{i3}^H \alpha_{m1} \mathbf{x}_{im} &= 0 \\
&\vdots \\
\mathbf{w}_{i1}^H \alpha_{mN} \mathbf{x}_{im} - \mathbf{w}_{iN}^H \alpha_{m1} \mathbf{x}_{im} &= 0 \\
\mathbf{w}_{i2}^H \alpha_{m3} \mathbf{x}_{im} - \mathbf{w}_{i3}^H \alpha_{m2} \mathbf{x}_{im} &= 0 \\
&\vdots \\
\mathbf{w}_{i,N-1}^H \alpha_{mN} \mathbf{x}_{im} - \mathbf{w}_{N}^H \alpha_{m,N-1} \mathbf{x}_{im} &= 0
\end{aligned}$$

Rewriting the above equations in a matrix form, we have

$$\tilde{\mathbf{X}}_{im}\mathbf{w}_i = \mathbf{0}, \tag{29}$$

where $\mathbf{w}_i \triangleq [\mathbf{w}_{i1}^H, \mathbf{w}_{i2}^H, \cdots, \mathbf{w}_{iN}^H]^H$ and the matrix $\tilde{\mathbf{X}}_m$ is defined as

$$\tilde{\mathbf{X}}_{im} \triangleq \begin{bmatrix} \tilde{\mathbf{x}}_{im1}^H & -\tilde{\mathbf{x}}_{im2}^H & 0 & \dots & \dots & 0 \\ \tilde{\mathbf{x}}_{im1}^H & 0 & -\tilde{\mathbf{x}}_{im3}^H & & & \vdots \\ \vdots & 0 & 0 & \ddots & & \vdots \\ \vdots & & & & \ddots & 0 \\ \tilde{\mathbf{x}}_{im1}^H & 0 & \dots & \dots & 0 & -\tilde{\mathbf{x}}_{imN}^H \\ 0 & \tilde{\mathbf{x}}_{im2}^H & -\tilde{\mathbf{x}}_{im3}^H & 0 & \dots & 0 \\ 0 & \tilde{\mathbf{x}}_{im2}^H & 0 & -\tilde{\mathbf{x}}_{im4}^H & \ddots & \vdots \\ 0 & \vdots & \vdots & \ddots & \ddots & 0 \\ 0 & \tilde{\mathbf{x}}_{im2}^H & 0 & \dots & 0 & -\tilde{\mathbf{x}}_{imN}^H \\ 0 & 0 & \tilde{\mathbf{x}}_{im3}^H & -\tilde{\mathbf{x}}_{im4}^H & 0 & 0 \\ \vdots & \vdots & \vdots & \vdots & \vdots & \vdots \\ 0 & 0 & 0 & 0 & \tilde{\mathbf{x}}_{im,N-1}^H & -\tilde{\mathbf{x}}_{imN}^H \end{bmatrix}, \tag{30}$$

and $\tilde{\mathbf{x}}_{imj} \triangleq \alpha_{mk}\mathbf{x}_{im}$ and $\tilde{\mathbf{x}}_{imk} \triangleq \alpha_{mj}\mathbf{x}_{im}$ for a given pair (j,k). Combining all symbols gives

$$\mathbf{X}_i\mathbf{w}_i = \mathbf{0}, \tag{31}$$

where the matrix $\mathbf{X}_i$ is defined as

$$\mathbf{X}_i \triangleq \begin{bmatrix} \tilde{\mathbf{X}}_{i1} \\ \tilde{\mathbf{X}}_{i2} \\ \vdots \\ \tilde{\mathbf{X}}_{iM_i} \end{bmatrix}. \tag{32}$$

The uniqueness of the solution and the identifiability of the proposed method is given by the following theorem.

Theorem 1 (Identifiability) For a class of interpolation functions which satisfy a complexity condition, the matrix $\mathbf{X}_i$ is a tall matrix with rank N^2-1, equivalently, the column rank is deficient by one for noiseless cases. Hence the $\mathbf{w}_i$ is the unique null space of $\mathbf{X}_i$. Hence Γ_i^{-1} is identifiable up to a scale factor. Proof: See Appendix.

By Theorem 1, we have

$$\Gamma_i^{-1} = \beta \mathbf{W}_i^H, \tag{33}$$

where β is a unknown scale factor. The estimate for the matrix $\mathbf{G}_i^\dagger$(pseudo-inverse) is directly given by

$$\mathbf{G}_i^\dagger = \beta \mathbf{W}_i^H \mathbf{U}_i^H. \tag{34}$$

The unknown scale factor β can be determined using only one pilot symbol placed at an arbitrary position within slot. An explicit channel parameter can be obtained by inversion. The inversion gives a perfect channel parameter at estimating points for noiseless cases. The channel at a specific symbol interval is obtained by (9). However, for the noisy case, the accuracy of the inverse depends on the condition number of $\mathbf{G}_i$. The inversion gives a reasonable performance for a well conditioned $\mathbf{G}_i$.

B.2 Noisy Observation

For the noisy case, the decorrelator output $\mathbf{z}_{im}$ is given by (20). Due to the additive noise, (31) is not satisfied exactly and the perfect channel identification is impossible in this case. We consider the following suboptimal approach. First, the range space of $\mathbf{G}_i$ is estimated by subspace decomposition of $\mathbf{Z}_i$ constructed as in (23) using noisy observations. With the estimated subspace, we formulate a least squares solution for (31).

Consider $\mathbf{Z}_i\mathbf{Z}_i^H$ and its expectation which are given by

$$\begin{aligned} \mathbf{Z}_i\mathbf{Z}_i^H &= \sum_{m=1}^{M_i} [\mathbf{G}_i |s_{im}|^2 \mathbf{a}_m \mathbf{a}_m^H \mathbf{G}_i^H + \mathbf{n}_{im}\mathbf{n}_{im}^H \\ &\quad + \mathbf{G}_i \mathbf{a}_m s_{im} \mathbf{n}_{im}^H + \mathbf{n}_{im}\mathbf{a}_m^H s_{im}^* \mathbf{G}_i^H] \qquad (35) \\ \mathbb{E}\{\mathbf{Z}_i\mathbf{Z}_i^H\} &= \mathbf{G}_i \Big(\sum_{m=1}^{M_i} |s_{im}|^2 \mathbf{a}_m \mathbf{a}_m^H\Big) \mathbf{G}_i^H + \sigma^2 \mathbf{\Sigma}_i \qquad (36) \end{aligned}$$

where $\mathbf{\Sigma}_i = \sum_{m=1}^{M_i} \mathbf{\Sigma}_{im}$. The subspace of $\mathbf{G}_i$ can be obtained by singular value decomposition of the whitened expectation of $\mathbf{Z}_i\mathbf{Z}_i^H$ as

$$\begin{aligned} \tilde{\mathbf{U}}_i \tilde{\mathbf{S}}_i \tilde{\mathbf{U}}_i^H &= \mathbf{\Sigma}_i^{-1/2} \mathbb{E}\{\mathbf{Z}_i\mathbf{Z}_i^H\} \mathbf{\Sigma}_i^{-H/2} \qquad (37) \\ \mathbf{U}_i &= \mathbf{\Sigma}_i^{1/2} \tilde{\mathbf{U}}_i \qquad (38) \end{aligned}$$

where $\sigma^2\mathbf{\Sigma}_i = \mathbf{\Sigma}_i^{1/2}\mathbf{\Sigma}_i^{H/2}$ is the Cholesky decomposition of $\sigma^2\mathbf{\Sigma}_i$. An estimate $\hat{\mathbf{U}}_i$ is obtained substituting $\mathbf{Z}_i\mathbf{Z}_i^H$ into the true expectation in (37). Since the noise $\mathbf{n}_{im}$ has zero

mean and is independent, the noise effect in (35) is averaged out and the approximation gives an accurate result for a large slot size which is our case.

With the estimated subspace, the projection $\mathbf{x}_{im}$ is given by

$$\mathbf{x}_{im} = \hat{\mathbf{U}}_i^H \mathbf{z}_{im} = \hat{\mathbf{U}}_i^H \mathbf{U}_i \Gamma_i \mathbf{a}_m s_{im} + \hat{\mathbf{U}}^H \mathbf{n}_{im}, \tag{39}$$

where the noise vector $\mathbf{U}^H \mathbf{n}_{im}$ has zero mean and covariance $\sigma^2 \hat{\mathbf{U}}^H \mathbf{\Sigma}_{im} \hat{\mathbf{U}}$. Assuming that $\hat{\mathbf{U}}_i^H \mathbf{U}_i$ is an identity[5], we can formulate a least squares solution for (31) which minimizes the following cost

$$\mathcal{E} = ||\mathbf{X}_i \mathbf{w}_i||^2, \tag{40}$$

under the constraint $||\mathbf{w}_i||^2 = 1$ which ensures a nontrivial solution. Specifically, the least square solution $\hat{\mathbf{w}}_i$ is given as

$$\hat{\mathbf{w}}_i = \arg\min_{||\mathbf{w}_i||=1} ||\mathbf{X}_i \mathbf{w}_i||^2 = \arg\min_{||\mathbf{w}_i||=1} \mathbf{w}_i^H \mathbf{X}_i^H \mathbf{X}_i \mathbf{w}_i \tag{41}$$

The solution of the above optimization is well known and given by the eigenvector associated to the smallest eigenvalue of $\mathbf{X}_i^H \mathbf{X}_i$.

In noisy case, the performance of our estimator based on the cross referencing depends on the noise power and its enhancement. The level of noise enhancement is dependent on the conditioning of the code matrix $\mathbf{T}$ and parameter matrix $\mathbf{G}_i$ which can be controlled by a proper selection of the number of users in the model K' and the number of estimating points N. Obviously the proposed two-step approach for the noisy case is not optimal. For a large slot size, however, the proposed subspace estimation and the least square solution based on it gives a good result. The overall performance of the proposed algorithm is evaluated through the comparison with Cramér-Rao bound and the Monte-Carlo simulations in Section V.

C. Detection

In this section, we propose new detection schemes for fast fading long code CDMA systems based on the proposed estimation method with the decorrelating front end.

[5]Since $\mathbf{\Sigma}_i$ is the sum of $\mathbf{\Sigma}_{im}$, $m = 1, \cdots, M_i$, it is almost an identity matrix for a large slot size. The whitening doesn't affect the performance much.

Once the decorrelation is performed at the front end, $\mathbf{z}_{im}$ forms a sufficient statistic for the detection of s_{im}. That is, after the decorrelation, all information relevant to the decision of symbol s_{im} is contained in $\mathbf{z}_{im}$ given by

$$\mathbf{z}_{im} = \mathbf{h}_{im} s_{im} + \mathbf{n}_{im} = \mathbf{G}_i \mathbf{a}_m s_{im} + \mathbf{n}_{im}, \tag{42}$$

where $\mathbf{n}_{im} \sim \mathcal{N}(\mathbf{0}, \sigma^2 \mathbf{\Sigma_{im}})$. Using the estimated channel, the maximum likelihood detector is the whitened RAKE receiver given by

$$\begin{aligned} \hat{s}_{im} &= \arg\min_{s_{im} \in \mathcal{C}} ||\hat{\mathbf{h}}_{im}^H \mathbf{\Sigma}_{im}^{-1} \mathbf{z}_{im} - s_{im}|| \\ &= \arg\min_{s_{im} \in \mathcal{C}} ||\mathbf{a}_m^H \hat{\mathbf{G}}_i^H \mathbf{\Sigma}_{im}^{-1} \mathbf{z}_{im} - s_{im}||, \end{aligned} \tag{43}$$

where $\mathcal{C}$ is the constellation. Even if the whitened RAKE gives an optimal detection, obtaining $\hat{\mathbf{h}}_{im}$ requires an additional matrix inversion since the proposed method gives an estimate of $\mathbf{G}_i^\dagger$. We propose the following suboptimal detection which utilizes the matrix $\mathbf{G}_i^\dagger$ directly as

$$\hat{s}_{im} = \arg\min_{s_{im} \in \ \mathcal{C}} ||\mathbf{a}_m^H \widehat{\mathbf{G}_i^\dagger} \mathbf{z}_{im} - s_{im}||, \tag{44}$$

where $\widehat{\mathbf{G}_i^\dagger}$ is the estimate of $\mathbf{G}_i^\dagger$. With a perfect estimate of $\mathbf{G}_i^\dagger$, the above method gives a zero-forcing equalizer followed by maximal ratio combining for given observation $\mathbf{z}_{im}$. It is well known that the zero-forcing solution usually gives a poor performance at low SNR due to noise enhancement. This can be mitigated by regularizing the direct inversion. The regularized least squares equalizer is given by

$$\mathbf{R}_i \triangleq (\mathbf{G}_i^H \mathbf{\Sigma}_{im}^{-1} \mathbf{G}_i + \sigma^2 \mathbf{I})^{-1} \mathbf{G}_i^H \mathbf{\Sigma}_{im}^{-1}. \tag{45}$$

For the case that $\mathbf{G}_i$ is a square matrix, (45) can be implemented using $\mathbf{G}_i^\dagger$ directly as

$$\mathbf{R}_i = \mathbf{G}_i^\dagger \mathbf{\Sigma}_{im}^{1/2} \left[\sigma^2 \mathbf{\Sigma}_{im}^{H/2} (\mathbf{G}_i^\dagger)^H \mathbf{G}_i^\dagger \mathbf{\Sigma}_{im}^{1/2} + \mathbf{I} \right]^{-1} \mathbf{\Sigma}_{im}^{-1/2}, \tag{46}$$

where $\mathbf{\Sigma}_{im} = \mathbf{\Sigma}_{im}^{1/2} \mathbf{\Sigma}_{im}^{H/2}$ is Cholesky factorization of $\mathbf{\Sigma}_{im}$. The proposed detector is given as

$$\hat{s}_{im} = \arg\min_{s_{im} \in \ \mathcal{C}} ||\mathbf{a}_m^H \hat{\mathbf{R}}_i \mathbf{z}_{im} - s_{im}||. \tag{47}$$

When $\mathbf{G}_i$ is not square, we can replace the regularized equalizer by $\mathbf{R}_i'$ defined as

$$\mathbf{R}_i' \triangleq \mathbf{G}_i^\dagger [\sigma^2 (\mathbf{G}_i^\dagger)^H \mathbf{G}_i^\dagger + \mathbf{I}]^{-1} \mathbf{\Sigma}_{im}^{-1}. \tag{48}$$

Here, (48) is obtained by setting the noise covariance $\mathbf{\Sigma}_{im}$ to an identity matrix inside inversion in (45) which is a reasonable approximation when spreading gain is high. Note that in (46) and (48) the knowledge of $\mathbf{G}_i$ and the direct inversion of $\mathbf{G}_i^\dagger$ are not required. Instead, the inversion of $\sigma^2(\mathbf{G}_i^\dagger)^H\mathbf{G}_i^\dagger + \mathbf{I}$ gives a stable algorithm even for the case of ill-conditioned $\mathbf{G}_i^\dagger$ due to the additive term.

D. Complexity

The complexity of the proposed method comes mainly from the channel estimation algorithm. We focus on the computational complexity of the proposed channel estimation. The overall procedure of the proposed estimator consists of the front end processing and two subspace decompositions to obtain the range of $\mathbf{G}_i$ and the null space of $\mathbf{X}_i$.

The code matrix defined in (7) is usually very large for long code CDMA. For a system with K users with equal spreading factor G, slot size M, and channel length L, the size of the code matrix is approximately $GM \times LMK$. The direct implementation of the matrix inversion required for the decorrelating and the regularized decorrelating front end is prohibitive in long code CDMA. However, the code matrix is highly structured and sparse. The number of nonzero entries of $\mathbf{T}$ is approximately $GMLK$. The fraction of nonzero elements is $1/M$ which is only several % of its entries for a large slot size. The direct inversion of the code matrix will lose the structure and the sparsity of the code matrix. The required matrix inversion can be implemented in an efficient way using a state-space technique. The computational complexity of the state-space inversion is in the order of GML^2K^2 which is linear with respect to the slot size M [13] . On the other hand, the conventional matched filter front end requires $GMLK$ computations which is the same number as the nonzero entries in the code matrix.

The subspace of $\mathbf{G}_i$ is obtained by matrix multiplication and singular value decomposition. Since the size of $\mathbf{Z}_i$ is $L \times M$, the matrix multiplication of $\mathbf{Z}_i\mathbf{Z}_i^H$ requires $2L^2M$ operations. The complexity of singular value decomposition of $\mathbf{Z}_i\mathbf{Z}_i^H$ is in order of L^3 which is not significant since L is small. The least squares solution of (41) is obtained by eigendecomposition of $\mathbf{X}_i^H\mathbf{X}_i$ where the size of $\mathbf{X}_i$ is $\frac{MN(N-1)}{2} \times N^2$. Due to the special sparse structure of $\mathbf{X}_i$, the computation of $\mathbf{X}_i^H\mathbf{X}_i$ requires at most $2M(N-1)N^4$ operations since only $M(N-1)$ elements are nonzero at each column of $\mathbf{X}_i$. The eigendecomposition

of $\mathbf{X}_i^H \mathbf{X}_i$ has the complexity order of N^6. For a system with reasonable parameters as in Section V-A, the computational complexity of the subspace decompositions is negligible compared with the decorrelating front end. For the case of the conventional matched filter, the computation required for the subspace decompositions is comparable to the front end processing. So, the processing for the proposed blind algorithm does not increase the computational complexity significantly in addition to the front end which is necessary for CDMA itself.

IV. Performance Analysis

A. Bit error rate

We present a brief analysis of the bit error rate (BER) of the proposed algorithm primarily focused on the whitened matched filter and the detector with the regularized equalizer in (47) using the decorrelating front end with BPSK signaling. For QPSK systems, the same technique can be used to obtain the symbol error rate (SER).

The decorrelating front end separates users in a deterministic and channel independent way, which makes the bit error rate analysis local to each user. However, the channel estimate and bit error are coupled in our case since blind channel estimators are also dependent on transmitted symbols. The coupling between channel estimate and bit error makes the direct analysis intractable. A reasonable approach is to evaluate the error rate of incoming bits conditioned on the current channel realization which shows an accurate performance in our simulation. Since the bit error rate changes symbol to symbol in time-varying channels, we calculate the error probability for each symbol with BPSK and average the error rate over slot period. Specifically, for user i, conditioned on the estimate $\hat{\mathbf{h}}_{im}$, the whitened RAKE detector gives a detected symbol as

$$\hat{s}_{im} = sgn(real(\hat{\mathbf{h}}_{im}^H \Sigma_{im}^{-1} \mathbf{z}_{im})). \tag{49}$$

For user i using BPSK with complex noise power σ^2 and bit energy E_i, the conditional bit error probability for the mth symbol is given by

$$\Pr(s_{im} \neq \hat{s}_{im}) = Q(\gamma_{im} \sqrt{\frac{2E_i}{G\sigma^2}}), \tag{50}$$

where $Q(\cdot)$ is the tail integral of the standard normal distribution, and γ_{im} is the loss factor with respect to the ideal BPSK signaling which is given by

$$\gamma_{im} \triangleq \frac{real(\hat{\mathbf{h}}_{im}^H \Sigma_{im}^{-1} \mathbf{h}_{im})}{\sqrt{\hat{\mathbf{h}}_{im}^H \Sigma_{im}^{-1} \hat{\mathbf{h}}_{im}}}. \tag{51}$$

For the case of orthogonal codes and perfect channel estimate, γ_{im} becomes one and (50) reduces to the ideal BPSK. The average bit error rate for a whole slot is given by

$$\bar{P}_i = \frac{1}{M_i} \sum_{m=1}^{M_i} \mathbb{E}\{Q(\gamma_{im} \sqrt{\frac{2E_i}{G\sigma^2}})\}, \tag{52}$$

where the expectation is taken over all channel estimate $\hat{\mathbf{h}}_{im}$.

Now consider the bit error performance of the detector using $\widehat{\mathbf{G}_i^\dagger}$ directly. Since the analysis is still local to each user and symbol, the bit error rate is given similarly as in the whitened RAKE receiver with change of loss factor γ_{im}. The new loss factor is given by

$$\gamma'_{im} \triangleq \frac{real(\mathbf{a}_m^H \hat{\mathbf{R}}_i \mathbf{h}_{im})}{\sqrt{\mathbf{a}_m^H \hat{\mathbf{R}}_i \Sigma_{im} \hat{\mathbf{R}}_i^H \mathbf{a}_m}}, \tag{53}$$

where $\hat{\mathbf{R}}_i$ is given in (46) or (48). The average bit error rate for whole slot is given by substituting γ'_{im} in (52) and taking expectation over all estimates of $\hat{\mathbf{R}}_i$.

V. Simulation

We present some simulation results to validate the proposed algorithm. For channel estimation, the mean square error (MSE) was used as the performance criterion. The estimation error of the proposed method consists of two components. The first is the error due to the channel modeling using interpolation with finite sample points[6]. The other error results from noise which characterizes the performance of the method itself. To separate the modeling error from the algorithm performance, we first generated a channel according to the interpolation model and assessed the MSE performance using Cramer-Rao bound and Monte-Carlo runs. The overall performance of the proposed method was also evaluated for lowpass channel with Jakes's spectrum. For symbol detection, symbol error rate (SER) was estimated using Monte Carlo simulation and was compared with the analytical calculation in Section IV-A.

[6]The perturbation to interpolation due to the noisy samples and truncation is well analyzed in [21].

A. Setup

We considered single and three QPSK users with equal power. Since our model was deterministic, the channel and spreading codes were randomly generated once and fixed throughout the Monte Carlo runs. When we evaluated the MSE of the channel estimator, the transmitted symbols were also fixed. In evaluating the SER, channels and spreading codes were fixed and the transmitted bits were generated randomly in each Monte Carlo run. The performance would vary with different channel and spreading parameters, but the qualitative behavior remains the same in various trials.

The spreading codes were pseudo-random sequences with spreading gain $G = 16$. The channel for each user had $L = 4$ fingers each of which had the same average magnitude. The relative delay offset for the single user case was $D = [0, 4, 8, 12]$ chips. The slot size was $M = 200$ symbols, and one pilot symbol was included at the beginning of the slot of each user to resolve the scale factor ambiguity of the blind estimator. We examined various linear interpolation techniques including piecewise linear, polynomial, ideal lowpass, optimal time-invariant, and optimal time-varying function[7]. The signal-to-noise ratio (SNR) was defined by E_b/σ^2 where the bit energy $E_b = avg(||\mathbf{h}_{im}||^2)GE_c$, E_c the chip energy, $avg(||\mathbf{h}_{im}||^2)$ is the average squared norm of channel vector over slot, and σ^2 the chip noise variance. More specific parameters used in the simulations can be found in [14].

B. MSE and BER Performance

The figure 3 shows the MSE performance of the proposed estimator with the decorrelating front-end for the single user system where the channel was generated according to the interpolation model with three estimating points and sinc coefficients. The channel vector at each estimating point was generated randomly and the Cramér-Rao bound in figure 3 is the semi-blind bound obtained using one pilot symbol in the slot front [15]. As shown in the figure, the proposed method closely follows the Cramér-Rao bound in the absence of channel modeling error. Since the channel at each estimating point was generated randomly, the matrix $\mathbf{G}_i$ was well conditioned and the inversion to obtain explicit $\hat{\mathbf{h}}_{im}$ did not contribute to inaccuracy much.

[7]Optimal interpolation function can be obtained as in [19] with the knowledge of spectral density of channel waveform.

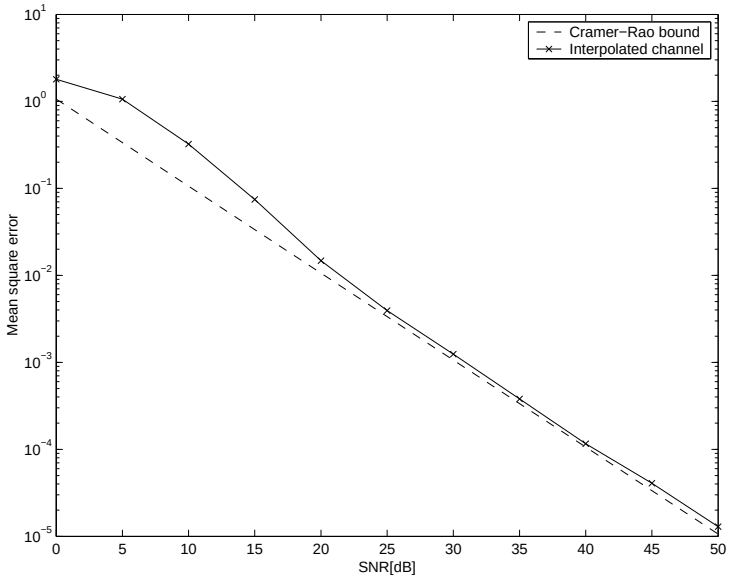

Fig. 3. Mean square error: interpolated channel

Figure 4 shows the SER performance for the single user system with the decorrelating front end using the same channel as figure 3. The RAKE receiver with the proposed channel estimate showed better performance than the proposed detector in (47) even with additional inversion. This is due to the scale factor associated with the blind method. Since the pilot symbol gave a known column in $\mathbf{G}_i$, the scale factor was resolved using $\mathbf{G}_i^\dagger \mathbf{G}_i = \mathbf{I}$. The scale factor obtained in this way resulted in more error than the required inversion of $\mathbf{G}_i^\dagger$ in the RAKE receiver where we first inverted $\mathbf{G}_i^\dagger$ and resolved the scale factor. However, the detector in (47) with a different scale factor estimated using one column of $\mathbf{G}_i^\dagger$ showed better performance than DRR at low and medium SNR. The zero-forcing detector scheme in (44) showed worse performance than (47) due to the noise enhancement. We also observed that the analytic BER calculations (51,52,53) were close to the performance obtained via Monte Carlo runs, indicating that the assumptions made in Sec. IV-A are accurate.

Figure 5 shows the MSE performance of the proposed algorithm for the single user system with a lowpass channel and the same other parameters described in section V-A. We compared the proposed method with the block fading model and a tracking method based on the previous decisions. The lowpass channel was generated according to Jakes's model with fading rate $f_D T_{slot} = 0.75$. This fading rate corresponds to 55 mi/h vehicle

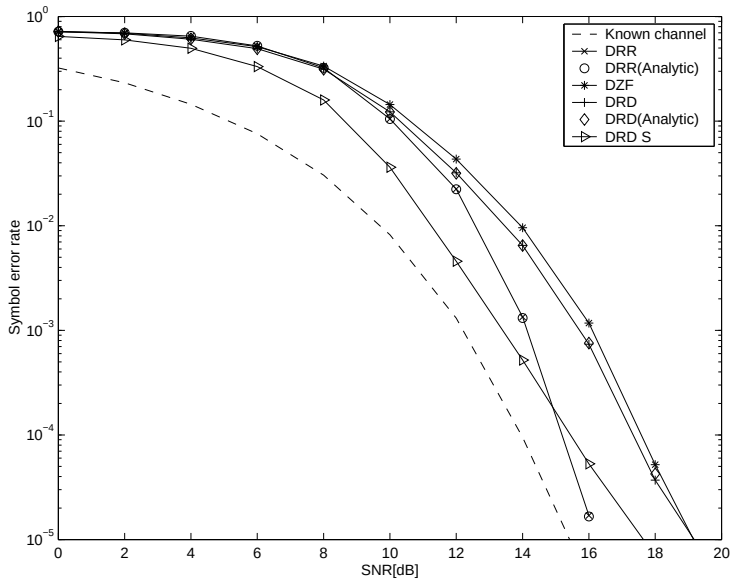

Fig. 4. Bit error rate: single user with interpolated channel - DRR: RAKE receiver with the proposed method with decorrelating front end, DZF: New detector using (44), DRD: New detector using (47 48), DRD S: scale factor using the true $\mathbf{G}^{\dagger}$

speed, the carrier frequency of 1.8 GHz and the slot size of 5 ms. For the decision based tracking scheme, we put a preamble of size W symbols in front of the slot and estimated the channel using least squares assuming the channel was constant over the interval of W symbols. Using the estimated channel, the next symbol was detected by RAKE receiver with the conventional matched filter and the estimation window was shifted by one symbol using the decision. We estimated the channel using the shifted window and repeated this procedure until the end of slot. We selected several window sizes and compared their performances. For the proposed blind method, we chose three estimating points at two ends and the middle of the slot and used the optimal time-varying interpolation coefficients. As expected, the proposed method gave better performance over the block fading assumption due to the capability of estimation of other points within the slot. We also observed that the decision directed method with a well chosen window size gave a good performance. As shown in the figure, the decision based tracking method with 2 symbol window showed worse performance at low and medium SNR due to the noise since the proposed method utilized all slot data whereas the training based scheme used only 2 symbols. However, at high SNR where the noise effect was negligible, the decision

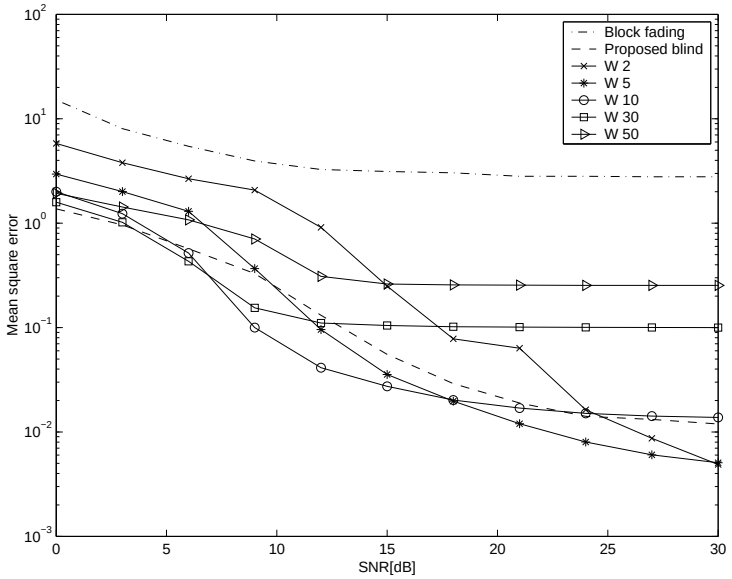

Fig. 5. Mean square error: single user with lowpass channel - Block fading assumption, the proposed estimation, the decision-directed tracking with window size W

based tracking showed better performance than the proposed method. For the window size of 5 symbols, the decision based method started to become better at a lower SNR than 2 symbol case. As we increased the window size, the performance of the decision directed tracking method degraded since the larger window was beneficial in point of SNR but it could not capture the time variation of the channel. Although it's not shown in the figure, other interpolation techniques such as piecewise linear and polynomial showed worse performance and sinc and optimal time-invariant were as good as optimal time-varying interpolation and frequency-domain approach also gave worse performance than time-domain approach with the same number of basis.

Figure 6 shows the symbol error performance for the single user system with the same lowpass channel as figure 5. The figure shows a similar trend to the MSE performance. The decision based method with a well chosen window size gives a good performance. The proposed blind method showed a comparable performance with the decision directed method with much less number of pilot symbols. However, for a large window, the decision directed method showed a performance floor due to the limitation in channel tracking.

Finally, fig. 7 shows the average SER performance for three user case using the decorrelating front end to separate users. The delay offset of each user from the slot reference

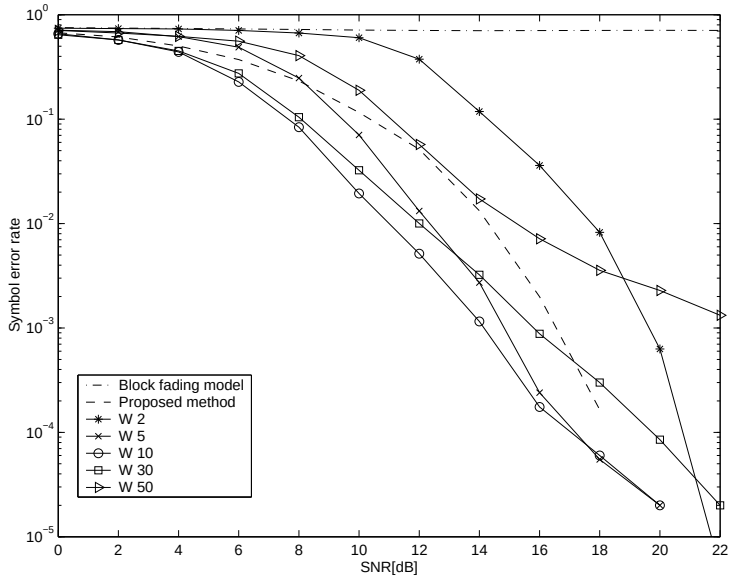

Fig. 6. Symbol error rate: single user with lowpass channel - Block fading assumption, RAKE with the proposed estimation, RAKE with the decision-directed tracking with window size W

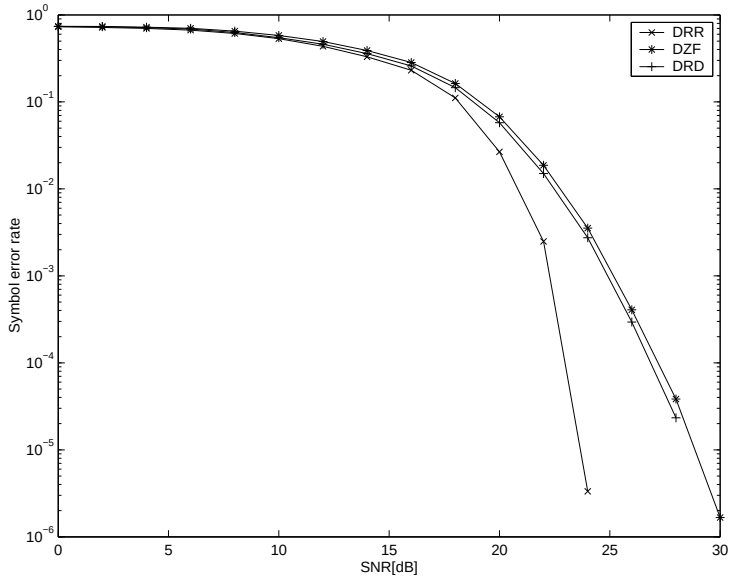

Fig. 7. Bit Error Rate: four users with low pass channel

was $D = [0, 8, 10]$ and the multipaths of a single user were delayed by one chip. Even if the relative behavior between the methods remained the same, the required SNR for the same error rate increased. This is due to the enhanced noise in (20) as the code matrix $\mathbf{T}$ becomes wider, which induces error in the cross reference cancellation.

VI. Conclusion

A new algorithm for the tracking of fast fading channels in long code CDMA systems is proposed by exploiting multipath diversity. Incorporating a linear interpolation model, the proposed method blindly estimates the channel coefficients at arbitrary estimating points within a slot and allows one pilot symbol for a transmitted block even with a larger size than the channel coherence time. The proposed method is useful in multipath rich environments and requires the rough knowledge of Doppler frequency of channel which can be obtained incorporating other Doppler frequency estimators. The computational complexity of the proposed method is not high compared with the front end processing. For multiuser case, the algorithm can be implemented efficiently using state-space inversion technique.

Appendix: Proof of theorem 1

Consider general modulation schemes such as M-PSK and QAM. Assume that $\alpha_{mn} \neq 0,\ n = 1, \cdots, N$ for given m, which is valid for most interpolation functions excluding the exact estimating points from observation symbols. Suppose that $\mathbf{w}_i$ satisfies (31). We can rewrite the equation as

$$\mathbf{w}_{ij}^H \mathbf{x}_{im}/\alpha_{mj} \quad = \quad \mathbf{w}_{ik}^H \mathbf{x}_{im}/\alpha_{mk},\ j \neq k, j, k = 1, \cdots, N$$

for $m = 1, \cdots, M$. Substituting $\mathbf{x}_{im} = \Gamma_i \mathbf{a}_m s_{im}$, we have

$$\mathbf{w}_{ij}^H \Gamma_i \mathbf{a}_m/\alpha_{mj} = \mathbf{w}_{ik}^H \Gamma_i \mathbf{a}_m/\alpha_{mk},\ j \neq k, j, k = 1, \cdots, N \tag{54}$$

since $s_{im} \neq 0$ for general modulation schemes. Rewriting (54) gives

$$\begin{aligned}(\mathbf{w}_{ij}^H \Gamma_i)_1 \frac{\alpha_{m1}}{\alpha_{mj}} + (\mathbf{w}_{ij}^H \Gamma_i)_2 \frac{\alpha_{m2}}{\alpha_{mj}} + \cdots + (\mathbf{w}_{ij}^H \Gamma_i)_j \\ + (\mathbf{w}_{i,j+1}^H \Gamma_i)_{j+1} \frac{\alpha_{m,j+1}}{\alpha_{mj}} + \cdots + (\mathbf{w}_{iN}^H \Gamma_i)_N \frac{\alpha_{mN}}{\alpha_{mj}}\end{aligned}$$

$$= (\mathbf{w}_{ik}^H \Gamma_i)_1 \frac{\alpha_{m1}}{\alpha_{mk}} + (\mathbf{w}_{ik}^H \Gamma_i)_2 \frac{\alpha_{m2}}{\alpha_{mk}} + \cdots + (\mathbf{w}_{ik}^H \Gamma_i)_k$$
$$+ (\mathbf{w}_{i,k+1}^H \Gamma_i)_{k+1} \frac{\alpha_{m,k+1}}{\alpha_{mk}} + \cdots + (\mathbf{w}_{iN}^H \Gamma_i)_N \frac{\alpha_{mN}}{\alpha_{mk}}, \quad (55)$$

where $(\cdot)_j$ represents the jth element of the vector. The above condition is satisfied for all $m = 1, \cdots, M$ $(M > 2N)$. For the class of interpolation functions which have such complexity that the ratios between coefficients α_{mn} in (55) form linearly independent columns, the necessary and sufficient condition is

$$(\mathbf{w}_{ij}^H \Gamma_i)_j = (\mathbf{w}_{ik}^H \Gamma_i)_k = \beta, \ \beta \text{ is a constant.} \quad (56)$$

$$(\mathbf{w}_{ij}^H \Gamma_i)_k = 0, \quad j \neq k, \quad (57)$$

which is equivalent to

$$\mathbf{W}_i^H \Gamma_i = \beta \mathbf{I}_N. \quad (58)$$

That is, $\mathbf{W}_i^H$ is the inverse of Γ_i. Since an inverse of a matrix is unique, $\mathbf{w}_i^H$ uniquely determined up to a scale factor. ■

References

[1] Fuyun Ling, "Optimal Reception, Performance Bound and Cutoff Rate Analysis of Reference-Assisted Coherent CDMA Communications with Applications," *IEEE Trans. Communications*, vol. 47, no. 10, pp. 1583-1592, Oct. 1999.

[2] J. K. Cavers, "An analysis of pilot symbol assisted modulation for Rayleigh fading channels," *IEEE Trans. Signal Processing* , vol. 40, no. 4, pp. 686 - 693, Nov. 1991.

[3] J. K. Cavers , "Pilot symbol assisted modulation and differential detection in fading and delay spread," *IEEE Trans. Communications*, vol.43, no.7, pp. 2206 - 2212, July 1995.

[4] H. Andoh, M. Sawahashi, and F. Adachi, "Channel estimation using time multiplexed pilot symbols for coherent RAKE combining for DS-CDMA mobile radio," *Proc. IEEE Intl. Symposium on Personal, Indoor and Mobile Radio Communications*, vol. 3, pp. 954-958, 1997.

[5] B. Lindoff, C. Ostberg, and H. Eriksson, "Channel estimation for the W-CDMA system, performance and robustness analysis from a terminal perspective," *Proc. IEEE Vehicular Technology Conference*, vol. 2, pp. 1565-1569, 1999.

[6] I. Sharfer and A. O. Hero, "Spread-spectrum sequence estimation and bit synchronization using an EM-type algorithm," *Proc. ICASSP*, vol. 3, pp. 1864-1867, 1995.

[7] E. Ertin, U. Mitra, and S. Siwamogsatham, "Maximum-likelihood based multipath channel estimation for code-division multiple-access systems," *IEEE Trans. Communications*, vol. 49, no. 2, pp. 290-302, Feb. 2001.

[8] X. Mestre and J. Fonollosa, "ML approaches to channel estimation for pilot-aided multirate DS/CDMA systems," *IEEE Trans. Signal Processing*, vol.3, no. 50, pp. 696-709, March 2002.

[9] S. Bhashyam and B. Aazhang, "Multiuser channel estimation and tracking for long code CDMA systems," *IEEE Trans. Communications*, vol. 50, no. 7, pp. 1081-1090, July 2002.

[10] A. Weiss and B. Friedlander, "Channel estimation for DS-CDMA downlink with aperiodic spreading codes," *IEEE Trans.Communications*, vol. COM-47, pp. 1561–1569, Oct 1999.

[11] Z. Xu and M. Tsatanis, "Blind channel estimation for long code multiuser CDMA systems," *IEEE Trans.Signal Processing*, vol. SP-48, pp. 988–1001, April 2000.

[12] C. Escudero, U. Mitra, and D. Slock, "A Toeplitz displacement method for blind multipath estimation for Long Code DS/CDMA signals," *IEEE Trans. Signal Processing*, vol. SP-48, pp. 654–665, March 2001.

[13] L. Tong, A. van der Veen, P. Dewilde, and Y. Sung, "Blind decorrelating rake receiver for long code WCDMA," *submitted to IEEE Trans. Signal Processing*, April 2002.

[14] Y. Sung and L. Tong, "Tracking of Fast-fading Channels in Long Code WCDMA," *Tech. Rep. ACSP-02-02*, Cornell University, Sep. 2002.

[15] Elisabeth De Carvalho and Dirk T. M. Slock , "Cramer-Rao bound for semi-blind, blind, and training sequence based channel estimation," *Proc. IEEE SP Workshop on SPAWC*, pp. 129-132 , Paris, April 1997.

[16] M. K. Tsatsanis and G. B. Giannakis, "Subspace methods for blind estimation of time-varying FIR channels," *IEEE Trans. Signal Processing*, vol.45, no.12, pp. 3084-3093, December 1997.

[17] D. Gesbert, P. Duhamel, and S. Mayrargue, "On-line blind multichannel equalization based on mutually referenced filters," *IEEE Trans. Signal Processing*, vol.45, pp.2307-2317, Sept. 1997.

[18] W. B. Davenport and W. L .Root, *An Introduction to the Theory of Random Signals and Noise.* McGraw-Hill, New York, N.Y., 1958.

[19] D. W. Tufts and N. Johnson, "Methods for Recovering a Random Waveform from a Finite Number of Samples," *IEEE Trans. Circuit Theory*, vol. CT-12, pp. 32-39, March 1965.

[20] G. Oetken, T. W. Parks, and H. W. Schüssler, "New Results in the Design of Digital Interpolators," *IEEE Trans. Acoustics, Speech, and Signal Processing*, vol.ASSP-23, no.3, pp.301-309, June 1975.

[21] R. J. Marks, *Introduction to Shannon sampling and interpolation theory.* Springer-Verlag, New York, NY, 1991.

[22] W. Jakes, *Microwave Mobile Communications.* Wiley, New York, 1974.